A multilevel formulation to simulate particulate flows

By S. V. Apte

1. Motivation and objectives

Many engineering problems involve two-phase flows, where particles of different shapes, sizes, and densities in the form of droplets, solid particles, or bubbles are dispersed in a continuum (gaseous or liquid) fluid. Numerical simulations of these flows commonly employ Lagrangian description for the dispersed phase and Eulerian formulation for the carrier phase. Depending on the volumetric loading of the dispersed phase two regimes are identified: dilute ($d_p << l$) and dense ($d_p \approx l$), where d_p is the particle diameter, and l the inter-particle distance. Furthermore, the grid resolution (Δ) used for solution of the carrier phase could be such that the particles are *subgrid* ($d_p << \Delta$) or *resolved* ($\Delta < d_p$) (cf. figure 1). Clearly, different numerical approaches are necessary to simulate various regimes of the flow. In addition, these regimes may occur in the same simulation, e.g. DNS or LES of wall-bounded turbulent flows with moderate particle loadings. Near the wall, the grid resolution in the wall-normal direction is extremely fine ($d_p > \Delta$) to capture the small scales of turbulence, and the particles move slowly thus increasing their residence time and number density near the wall and decreasing the inter-particle distance ($l \approx d_p$), whereas away from the wall the grid resolution is coarse and the inter-particle distance is large. A multi-level approach capable of addressing all regimes is needed.

Typical simulations involving millions of dispersed particles employ "point-particle" approach for dilute particle-loadings (Apte *et al.* 2003a; Apte *et al.* 2003b; Segura *et al.* 2004) where the forces on the dispersed phase are computed through model coefficients and the effect of particles on the carrier phase is represented by a force applied at the *centroid* of the particle. Although this approach has been shown to give good results for swirling, separated flows (Apte *et al.* 2003a), it fails to properly capture turbulence modulation in wall-bounded flows (Segura *et al.* 2004). If the volumetric loading is high or the particle size is greater than Kolmogorov scale, simple drag/lift laws for particle motion (used in the point-particle approach) do not capture the unsteady wake effects (Burton & Eaton 2003). Apte *et al.* (2003c) (henceforth CTR-ARB03) performed simulations of Poisuille flow with large spherical particles arranged in layers at the bottom of the channel. It was shown that the point-particle approach was unable to provide any lift to the particles in this shearing flow. Accounting for volumetric effects of the spherical particles was important to obtain lift and fluidization of the channel as observed in fully resolved DNS studies (Choi & Joseph 2001; Patankar *et al.* 2001). The formulation developed in Apte *et al.* (2003c) is applicable to dense as well as dilute regimes (here the effect of volume fraction will be negligible). However, it requires that the size of particles is *less* than the grid control volume.

If $d_p >> \Delta$, the particle-domain is completely resolved by the grid, and forces on the particle should be computed directly. A variety of approaches based on distributed Lagrange multipliers (DLM)/fictitious domain method (Glowinski *et al.* 1999; Patankar *et*

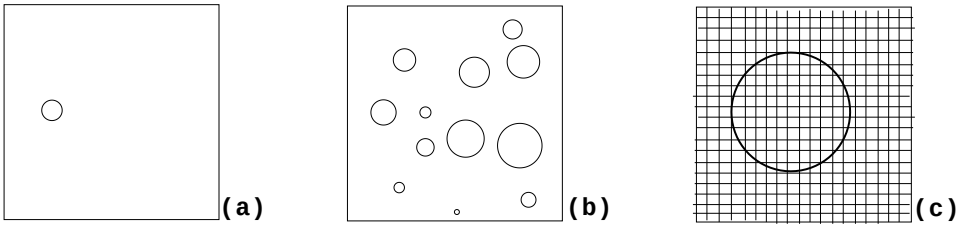

FIGURE 1. Regimes of particulate flows in Eulerian-Lagrangian simulations: a) dilute, b) dense, c) resolved

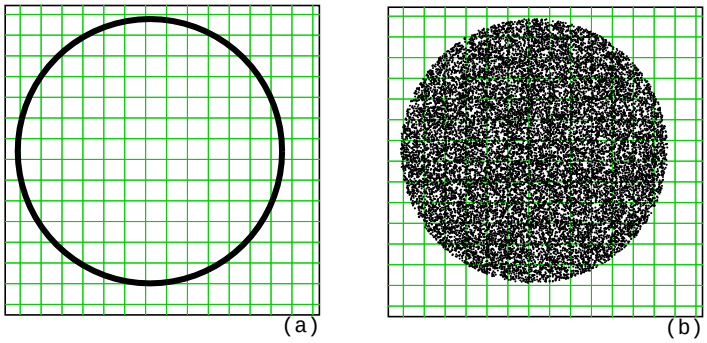

FIGURE 2. Use of material points to describe the particle domain: a) original sphere, b) sphere replaced by material points. Each material point has an associated volume (and thus a length scale) so that the total volume of all material points is equal to the original particle.

al. 2000), arbitrary Lagrangian-Eulerian (ALE) formulation (Hu *et al.* 2001), immersed boundary based direct forcing method (Kajishima & Takagi 2002), fast computation techniques based on DLM (Patankar 2001; Sharma & Patankar 2004) have been developed and applied to simulate these types of "resolved" particulate flows. For turbulent flow simulation of large number of particles, two approaches stand-out because of their easy implementation and fast computation: a) Kajishima & Takagi (2002) (henceforth KT02) and b) Patankar (2001). The formulation due to KT02 is explicit in terms of particle momentum coupling and is first-order accurate in time, however, has been shown to give good results for particle-turbulence interactions. Patankar (2001) developed a formulation which is implicit for particle momentum coupling. We attempt to extend the framework developed in CTR-ARB03 by investigating the resolved particle regime. The emphasis in this work is to develop a formulation for resolved particles, which can be directly used in conjunction with formulation described in CTR-ARB03, and thus can be used to compute all regimes encountered in particulate flows. We first investigate the formulation based on KT02 and propose modifications/improvements.

2. Governing equations

We assume that the particle size, d_p, is much larger than the grid spacing, Δ, as shown in figure (1c). We also assume that the particles are rigid. The grid used is kept fixed

and part of the control volumes occupy the particle domain. Following the notation used in CTR-ARB03, Θ_g and Θ_p represent the carrier and dispersed phase volume fractions, respectively, and $\Theta_p + \Theta_g = 1$. We define the composite velocity as,

$$\mathbf{u} = \Theta_g \mathbf{u}_g + (1 - \Theta_g)\, \mathbf{u}_p \tag{2.1}$$

where $\mathbf{u}_g$ is the fluid velocity vector, and $\mathbf{u}_p = \mathbf{U}_p + \omega_p \times \mathbf{r}$ the particle velocity. Here, $\mathbf{U}_p$ is the translational velocity and ω_p the angular velocity of rigid body rotation. Equation (2.1) represents the volume-weighted velocity at the interfacial control volumes. For no-slip and non-permeable interface, $\mathbf{u}_g = \mathbf{u}_p$, the Navier-Stokes equations for an incompressible fluid with rigid particles become:

$$\bigtriangledown \cdot \mathbf{u} = 0 \tag{2.2}$$

$$\rho_g(\frac{\partial \mathbf{u}}{\partial t} + \mathbf{u} \cdot \bigtriangledown \mathbf{u}) = - \bigtriangledown p + \mu_g \bigtriangledown \cdot \left(\bigtriangledown \mathbf{u} + (\bigtriangledown \mathbf{u})^T \right) + \rho_g \mathbf{g} + \mathbf{F} \tag{2.3}$$

where μ_g is the dynamic viscosity of fluid, $\mathbf{g}$ the gravitational force, and $\mathbf{F}$ the force acting to enforce the rigid-body motion within the particle domain. If the particle is moving with a velocity of $\mathbf{u}_p$, the fluid velocity inside the particle domain ($\Theta_p = 1$) should be $\mathbf{u} = \mathbf{u}_p$. The force imposing this condition is given as $\mathbf{F}_p = \rho_g(\mathbf{u}_p - \mathbf{u})/\Delta t$. In KT02, a first order approximation is used for the force in the region $0 < \Theta_p < 1$ to give,

$$\mathbf{F} = \rho_g \Theta_p \frac{\mathbf{u}_p - \mathbf{u}}{\Delta t} \tag{2.4}$$

This force is applied to the centroid of the grid control volumes. In this work, we present a better representation of the force to impose rigid body motion in the particle domain as shown below.

2.1. *Volume fraction and interphase force*

In order to compute the volume fraction (Θ_p) we replace each particle by N_m "material points" distributed over the entire particle domain as shown in figure 2. Each material point has an associated volume such that the total volume of the material points is equal to the particle volume. The centroid of a material point cannot be inside the volume of another. The volume fraction is easily obtained as

$$\Theta_p\,(\mathbf{x}) = \sum_{k=1}^{N_m} V_k \mathcal{G}_\sigma\,(\mathbf{x} - \mathbf{x}_k) \tag{2.5}$$

where the summation is over all material points N_m. Here $\mathbf{x}_k$ is the particle location, $\mathbf{x}$ the centroid of a control volume, and V_k the volume of each material point. The function $\mathcal{G}_\sigma$ is the interpolation operator given as

$$\mathcal{G}_\sigma(\mathbf{x}_p) = \frac{1}{\left(\sigma\sqrt{2\pi}\right)^3} exp\left[-\frac{\sum_{i=1}^{3} (x_i - x_{p,i})^2}{2\sigma^2} \right]. \tag{2.6}$$

The Gaussian interpolation operator is normalized to satisfy $\int_V \mathcal{G}_\sigma \left(\S - \S_\| \right) dV = 1$, where V is the grid control volume and the filter-width (σ) is proportional to the grid size. This enforces mass (or volume) conservation over the material points. It should be noted that, the particle surface is diffused by this procedure over a length-scale of the order of the grid spacing (Δ), and its effect on the flow is reduced with increased grid resolution. We believe that for the purpose of capturing unsteady wake effects in turbulent flows with many particles, this approximation is sufficient and is verified later. In KT02,

volume fraction is computed by approximating the sphere by a polygon enclosing the sphere and obtained by drawing tangents to the spherical surface in each control volume. In turn, the effective total volume of the sphere is increased. Similar, error is introduced at the particle interface.

The force acting on the fluid phase is given as

$$\mathbf{F}\left(\mathbf{x}\right) = \sum_{k=1}^{N_m} V_k \rho_g \mathcal{G}_\sigma \left(\frac{\mathbf{u}_{p,k} - \mathbf{u}}{\Delta t} \right). \tag{2.7}$$

This interpolation procedure gives a smoother force field near the particle surface. The main advantages of using Gaussian interpolation and material points are: a) the interphase force and volume fractions can be readily evaluated for *arbitrary* shaped particle, b) the material points move as a rigid body, thus they do not change their positions relative to each other and recomputing volume fraction field does not require any expensive computation of finding the intersections of particle surface with grid nodes, and c) same interpolation scheme was used to compute force and volume fraction in simulations of dilute and dense particulate flow (CTR-ARB03).

3. Numerical Algorithm

The above system of equations is solved using the fractional step algorithm on unstructured grids as described by Mahesh *et al.* (2004). The steps are summarized below:

- **Step 1:** Compute the volume fraction field using equation 2.5.
- **Step 2:** Advance the fluid momentum equations without the interphase force, $\mathbf{F}$.

$$\frac{\rho_g u_i^* - \rho_g u_i^n}{\Delta t} + \frac{1}{2V} \sum_{\text{facesofcv}} \left[u_{i,f}^n + u_{i,f}^* \right] g_N^{n+1/2} A_f = \frac{1}{2V} \sum_{\text{facesofcv}} \mu_f \left(\frac{\partial u_{i,f}^*}{\partial x_j} + \frac{\partial u_{i,f}^n}{\partial x_j} \right) A_f \tag{3.1}$$

where f represents the face values, N the face-normal component, $g_N = \rho_g u_N$, and A_f is the face area.

- **Step 3:** Compute the force on material points:

$$\mathbf{F}_{p|\mathbf{x}_{p,k}} = \rho_g \left(\frac{\mathbf{u}_p^n - \mathbf{u}_{\mathbf{x}_{p,k}}^*}{\Delta t} \right) \tag{3.2}$$

where $\mathbf{u}^*$ is interpolated to the material point k of a particle.

- **Step 4:** Project force from material points onto the grid control volume using equation 2.7.
- **Step 5:** Correct the velocity field within the particle domain by imposing the force:

$$\rho_g \widehat{u}_i = \rho_g u_i^* + F_i \Delta t \tag{3.3}$$

- **Step 6:** Interpolate the velocity fields to the faces of the control volumes and solve the Poisson equation for pressure:

$$\bigtriangledown^2 \left(p \Delta t \right) = \frac{1}{V} \sum_{\text{facesofcv}} \rho_g \widehat{u_{i,f}} A_f \tag{3.4}$$

- **Step 7:** Reconstruct the pressure gradient, compute new face-based velocities, and update the cv-velocities using the least-squares interpolation used by Mahesh *et al.*

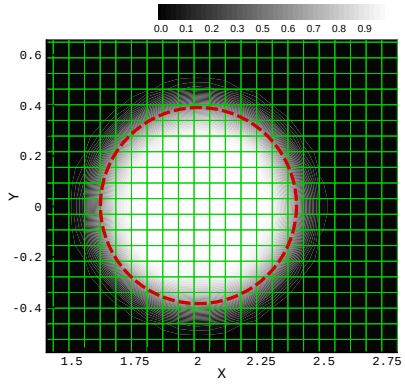

FIGURE 3. Distribution of particle volume fraction field for a single sphere on uniform grid.

(2004):

$$\frac{\rho_g \left(u_i^{n+1} - \widehat{u}_i\right)}{\Delta t} = -\frac{\partial p}{\partial x_i} \tag{3.5}$$

- **Step 8:** Advance the particle velocity. The total force $\mathbf{F}$ acting on a particle is simply the summation $(\sum_{k=1}^{N_m} \mathbf{F}_p V_k)$ over all material points. Similarly, torque acting at each material point is given as, $\mathbf{T} = \sum_{k=1}^{N_m} (\mathbf{F}_p \times \mathbf{r}_{p,k}) V_k$, where $\mathbf{r}_{p,k}$ is the position vector of the each material point from the particle centroid:

$$m_p u_{p,i}^{n+1} = m_p u_{p,i}^n - \Delta t F_{p,i} + m_p g_i \tag{3.6}$$

$$I_p \omega_{p,i}^{n+1} = I_p \omega_{p,i}^n - \Delta t T_{p,i} \tag{3.7}$$

where m_p is the particle mass, I_p the moment of inertia, $u_{p,i}$ and $\omega_{p,i}$ the particle translational and angular velocities, respectively.

- **Step: 9** Advance the particle positions:

$$x_{p,i}^{n+1} = x_{p,i}^n + \frac{\Delta t}{2}\left(u_{p,i}^n + u_{p,i}^{n+1}\right) \tag{3.8}$$

The above formulation is similar to the one given in KT02 with some key differences: a) we compute the volume fraction and force acting on the particle as described in section 2.1. The forces acting at the material points within each particle are interpolated onto the Eulerian grid by a Gaussian interpolation operator to give smoother representation of the field (see equation 2.7), b) the rigid body motion to the fluid velocity is imposed before the incompressibility constraint (KT02 impose Step 3 after solving the Poisson equation). This way the flowfield over the computational domain satisfies the incompressibility constraint exactly, however, rigid-body motion within the particle domain is imposed only approximately, and c) the volume fraction computation is applicable to any arbitrary shaped particle.

4. Results

We investigate the above formulation by simulating flow over a *fixed* sphere at different Reynolds numbers and compare the predicted drag coefficients with experimental data. The computational domain is a rectangular box of dimension $8 \times 8 \times 8\ m$ and the sphere

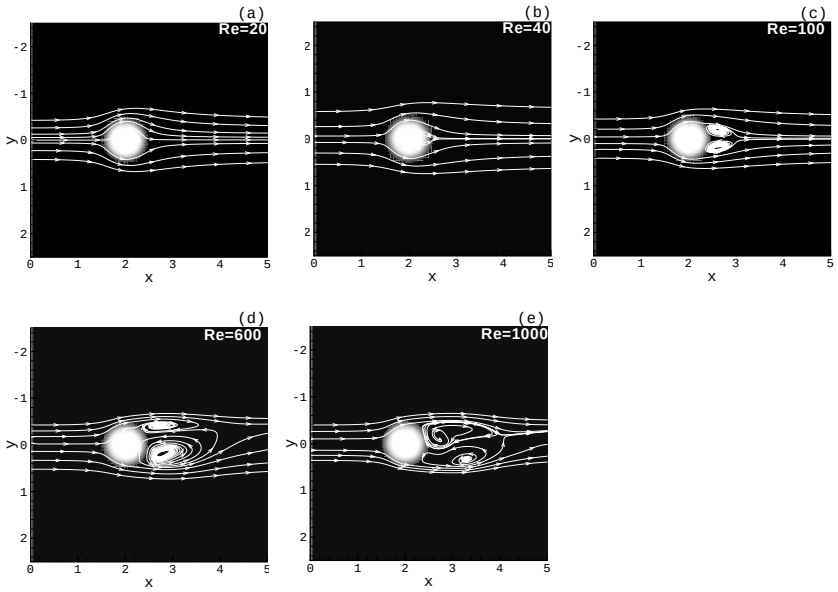

FIGURE 4. Instantaneous streamlines for flow over a stationary sphere at different Reynolds numbers: a) Re=20, b) Re=40, c) Re=100, d) Re=600, and e) Re=1000. Also shown are the contours of particle volume fraction, Θ_p.

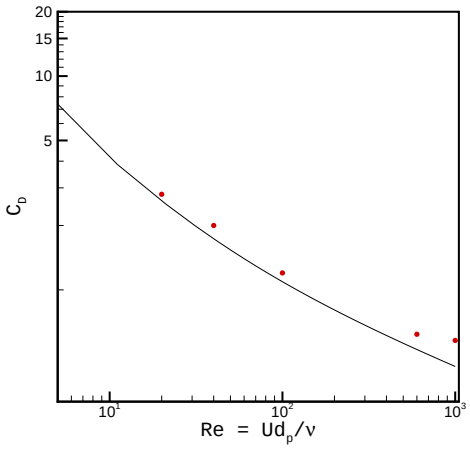

FIGURE 5. Comparison of drag coefficient for flow over a fixed sphere: ——— non-linear drag law Clift *et al.* (1978), ∘ present.

diameter is $d_p = 0.8\ m$ with its centroid located at [2,0,0]. The computational grid consists of uniform, cubic elements of size $128 \times 128 \times 128$ giving approximately 11 grid cells in each direction over the particle domain ($d_p/\Delta = 11$). We impose uniform fluid velocity at the inlet, convective boundary condition at the exit and periodic conditions in the y and z directions.

Figure 3 shows the distribution of particle volume fraction together with the sphere

surface. It shows that Θ_p is smoothed over the particle boundary and covers a domain larger than the actual particle size by one grid cell. Increased resolution reduces this spread. We used 5000 material points uniformly distributed over the particle domain to compute the volume fraction field, however, out tests indicate that fewer material points are enough to provide the volume fraction field. Flow over the fixed sphere was simulated at six different Reynolds numbers ($Re = \rho_g d_p U/\mu_g$) over a range of $20-1000$. The particle was fixed by specifying $\mathbf{u}_p^n = 0$ in Step 3 of the formulation and the equations for particle motion are not necessary (Steps 8 and 9). Figure 4 shows the instantaneous streamlines at different Reynolds numbers. The flowfield is symmetric for low Reynolds numbers and unsteady vortex shedding is observed for higher Reynolds numbers ($>$ 200). Figure 5 compares the drag coefficients at different Reynolds numbers with the experimental curve fit, $C_d = \frac{24}{Re}\left(1 + 0.15Re^{0.687}\right)$ obtained from Clift *et al.* (1978). The drag coefficient obtained from present simulations is within 5-15% of the experimental data with maximum error obtained at $Re = 1000$. Overprediction of drag is due to the spreading of the particle domain as shown in figure 3. Similar results have been reported in KT02.

5. Discussion

A formulation for simulating *resolved* particles ($d_p >> \Delta$) is developed based on the work by Kajishima & Takagi (2002). Regions where particles are *subgrid* ($d_p < \Delta$), can be captured by using the formulation developed in CTR-ARB03. Thus, different regimes encountered in particle-laden flows in the same simulation can be handled. The resolved particle domain is replaced by material points which do not move relative to each other. Forces acting at the material points are interpolated to the Eulerian grid using a Gaussian interpolation operator. It was observed that the present formulation predicts the drag on a fixed sphere correctly and captures unsteady wake effects with grid resolution (d_p/Δ) of the order 10.

Based on this work, a simple extension to the standard point-particle approach can be devised. In LES or DNS of particle-laden channel flows the typical grid resolution in the wall-normal direction is $3-10\ d_p$ (see Segura *et al.* 2004). With point-particle approach, all of the interphase force is applied at the particle centroid. In regions with high grid resolution, one may use material points to represent the particles. This will distribute the interphase force over a length scale comparable to the particle diameter. In addition, flow modification due to wake-effects can be captured by material points with sufficient grid resolution.

The formulation presented here is explicit for momentum coupling and first order accurate in time. The temporal accuracy can be increased by performing iterations per time-step over the fluid and particle equations, however, is costly. Explicit coupling is undesirable as it may give rise to instabilities and unphysical oscillations in drag/lift forces. As shown by Patankar 2001 (also Sharma & Patankar 2004) an implicit momentum coupling with little increase in computational time is possible and should be used. Our future effort will focus on combining the present approach with their implicit algorithm to develop a robust and accurate numerical scheme for simulations of particle/turbulence interactions in complex flows.

6. Acknowledgement

Discussions and communications with Prof. Neelesh Patankar (Northwestern University) are grately appreciated.

REFERENCES

APTE, S. V., MAHESH, K., MOIN, P., & OEFELEIN, J.C. 2003a Large-eddy simulation of swirling particle-laden flows in a coaxial-jet combustor. *Int. J. Mult. Flow* **29**, 1311-1331.

APTE, S. V., GOROKHOVSKI, M. & MOIN, P. 2003b LES of atomizing spray with stochastic modeling of secondary breakup *Int. J. Mult. Flow* **29**, 1503-1522.

APTE, S. V., MAHESH, K., & LUNDGREN, T. 2003c

BURTON, T. M. & EATON, J. K. 2003 Fully resolved simulations of particle-turbulence interaction. *Rep. No. TSD–151*, Dept. of Mech. Engr., Stanford University.

CLIFT, R., GRACE, J.R., & WEBER, M.E. 1978 Bubbles, drops, and particles. Academic Press, New York.

CHOI, H.G., & JOSEPH, D.D. 2001 Fluidization by lift of 300 circular particles in plane Poisuille flow by direct numerical simulation. *J. Fluid. Mech.* **438**, 101–128.

GLOWINSKI, R., PAN, T.-W., HESLA, T. I., & JOSEPH, D. D. 1999 A distributed Lagrange multiplier/fictitious domain method for particulate flows. *Int. J. Multiphase Flow* **25**, 755–794.

HU, H. H., PATANKAR, N. A., & ZHU, M. Y., 2001. Direct numerical simulations of fluid-solid systems using Arbitrary Lagrangian-Eulerian technique. *J. Comp. Phys.* **169**, 427–462.

KAJISHIMA, T., & TAKIGUCHI, S. 2002 Interaction between particle clusters and particle-induced turbulence. *J. Heat Fluid Flow*, **23**, pp. 639–646.

MAHESH, K., CONSTANTINESCU, G., & MOIN, P. 2004 A New Time-accurate Finite-Volume Fractional-Step Algorithm for Prediction of Turbulent Flows on Unstructured Hybrid Meshes. *J. Comp. Phy.* **197**, 215–240.

MOIN, P, & APTE, S.V. 2005 LES of multiphase reacting flows in complex combustors *AIAA J.* to appear.

PATANKAR, N. A. 2001b Lagrangian numerical simulation of particulate flows. *Int. J. Multi. Flow* **27**, 1685-1706.

PATANKAR, N. A., SINGH, P., JOSEPH, D. D., GLOWINSKI, R., & PAN, T.-W. 2000. A new formulation of the distributed Lagrange multiplier/fictitious domain method for particulate flows. *Phy. Fluids*, **9**, 3786–3807.

PATANKAR, N. A., HUANG, P. Y., KO, T., & JOSEPH, D. D. 2001 Lift-off of a single particle in Newtonian and viscoelastic fluids by direct numerical simulation, J. FLUID MECH. **438**, 67–100.

SHARMA, N., & PATANKAR, N. A. 2004 A fast computation technique for the direct numerical simulation of rigid particulate flows. *J. Comp. Phy.*, in press.

SEGURA, J. C., EATON, J. K. & OEFELEIN, J. C. 2004 Predictive capabilities of particle-laden LES. *Rep. No. TSD–156*, Dept. of Mech. Engng., Stanford University.